Chapter 3

Interaction of Strong Laser Fields with Matter

Ultrashort and intense laser radiation opens the door for a new class of nonlinear effects including above threshold ionisation (ATI) [Cor89], high harmonic generation (HHG) [Cor93], atomic stabilisation [PGa90], and molecular dissociation [SIC95]. Understanding ionisation mechanisms plays an important role for the explanation of these and other strong field effects. This chapter starts with a discussion of general aspects of strong field interactions. Then, direct ionisation and non-statistical fragmentation are considered. After that, redistribution of the absorbed energy in large but finite systems is discussed. Finally, the competing processes of statistical ionisation and fragmentation are revisited.

3.1 General Aspects

In context of the present work the electrical field strength of laser radiation applied to an object of interest is considered to be strong enough to induce significant modifications of its energy landscape. One relevant quantity is the ponderomotive energy. It describes the average oscillation energy that is acquired by a free electron in the radiation field of the laser pulse. The ponderomotive energy is given by the following equation

$$U_P = \frac{q^2}{2m_e\varepsilon_0 c\omega^2} I \quad , \tag{3.1}$$

where q is the electron charge, m_e is the mass of the electron, ε_0 is the dielectric constant in vacuum, c is the speed of light, ω is the angular frequency of the laser radiation, and I is the laser field intensity. The ponderomotive energy depends on the square of the wavelength and

is linearly dependent on the intensity, this can be numerically expressed as

$$U_P[\mathrm{eV}] = 9.34 \times 10^{-20} \times (\lambda[\mathrm{nm}])^2 \times I\left[\mathrm{W/cm^2}\right] \quad . \tag{3.2}$$

U_P can be used as a criterion to determine if a field is strong by comparison of the characteristic ionisation energy E_I of the system in question with U_P. For the ionisation process the strong field regime starts if

$$U_P > E_I \quad . \tag{3.3}$$

For example, the ionisation of C_{60} with $E_I = 7.58\,\mathrm{eV}$ [VSK92] by the laser radiation centred at $800\,\mathrm{nm}$ would be strong in this sense if $I > 1.3 \times 10^{14}\,\mathrm{W/cm^2}$.

The interaction of strong laser radiation with complex many-body systems can lead to substantial energy absorption. This process drives the system out of its equilibrium. After the energy is deposited into the system, relaxation occurs by the release of the excess energy. There are three relaxation mechanisms for a free molecule or cluster: ionisation, fragmentation, and photon emission in a form of fluorescence (transitions on the ns time scale from an excited singlet state to the ground state) or phosphorescence (transitions on the slower time scales from an excited metastable, usually triplet, state to the ground state). Ionisation and fragmentation are two most important mechanisms of excess energy release among them.

For ionisation the absorbed energy must be larger than the ionisation potential of the system. Direct and delayed ionisation can be distinguished. Direct ionisation is the electron emission which happens on the time scale of the laser pulse acting. Delayed ionisation is observed after the laser pulse passed. The latter has a statistical nature and occurs after equilibration among electronic degrees of freedom.

In principle, fragmentation happens when the internal vibrational energy is greater than the dissociation energy of the system. Unimolecular fragmentation occurs when the system separates into two or more parts. Usually, the initial system is called the "parent" and the fragments are called "daughters". Similar to ionisation, fragmentation may have non-statistical and statistical origin. Non-statistical fragmentation occurs on a time scale before complete energy equilibration among vibrational degrees of freedom. On the other hand, excitation of the molecule to a repulsive potential energy surface may lead to non-statistical fragmentation. Fragmentation due to multiple excitation of one particular vibrational mode until the amplitude of the vibration leads to dissociation is a non-statistical process as well. Experimentally, it can

be achieved either by laser radiation tuned to the vibrational frequency or in the temporal domain by exciting the system with a train of laser pulses.

3.2 Multiphoton Ionisation and Fragmentation

At low intensities, photoionisation can only occur if the energy of the absorbed photon $\hbar\omega$ is higher than the binding energy (or ionisation potential) E_I of an electron. In multiphoton ionisation (MPI) processes (see e.g. [PKK97, HSc08]) N photons of energy $\hbar\omega$ are absorbed and the energy balance is given by

$$E_K + E_{int} = N\hbar\omega - E_I \quad , \tag{3.4}$$

where E_K is the kinetic energy of the ejected electron and E_{int} is the internal rotational and vibrational energy of the system directly after the ionisation process. Here it is assumed that N is the minimum number of photons needed for an MPI process

$$N\hbar\omega \geq E_I \geq (N-1)\hbar\omega \quad . \tag{3.5}$$

If the electric field strength becomes comparable with the atomic Coulomb potential, the electron can tunnel through the potential barrier and leave the atom which is referred to as the tunnelling ionisation [ASM89].

The dependence of the ionisation probability on the ionisation potential and properties of the laser radiation (intensity I and frequency ω) was theoretically investigated by L. V. Keldysh [Kel65]. It was found that the MPI and the tunnelling ionisation are two limiting regimes of nonlinear ionisation. The Keldysh parameter γ was introduced to define the transition between these two different ionisation regimes

$$\gamma = \sqrt{\frac{E_I}{2U_P}} = \sqrt{\frac{\varepsilon_0 m_e c E_I \omega^2}{q^2 I}} \quad . \tag{3.6}$$

Assuming $\hbar\omega < E_I$, one can distinguish the MPI case if $\gamma > 1$ (ionisation with high frequency and rather low intensity), while tunnelling ionisation occurs if $\gamma \ll 1$ (ionisation with low frequency and high intensity). The evolution from MPI to tunnelling ionisation was observed experimentally [MBT93]. Often, these two limiting regimes are referred to as the the perturbative nonlinear regime and the strong-field regime, respectively. Alternatively, the Keldysh

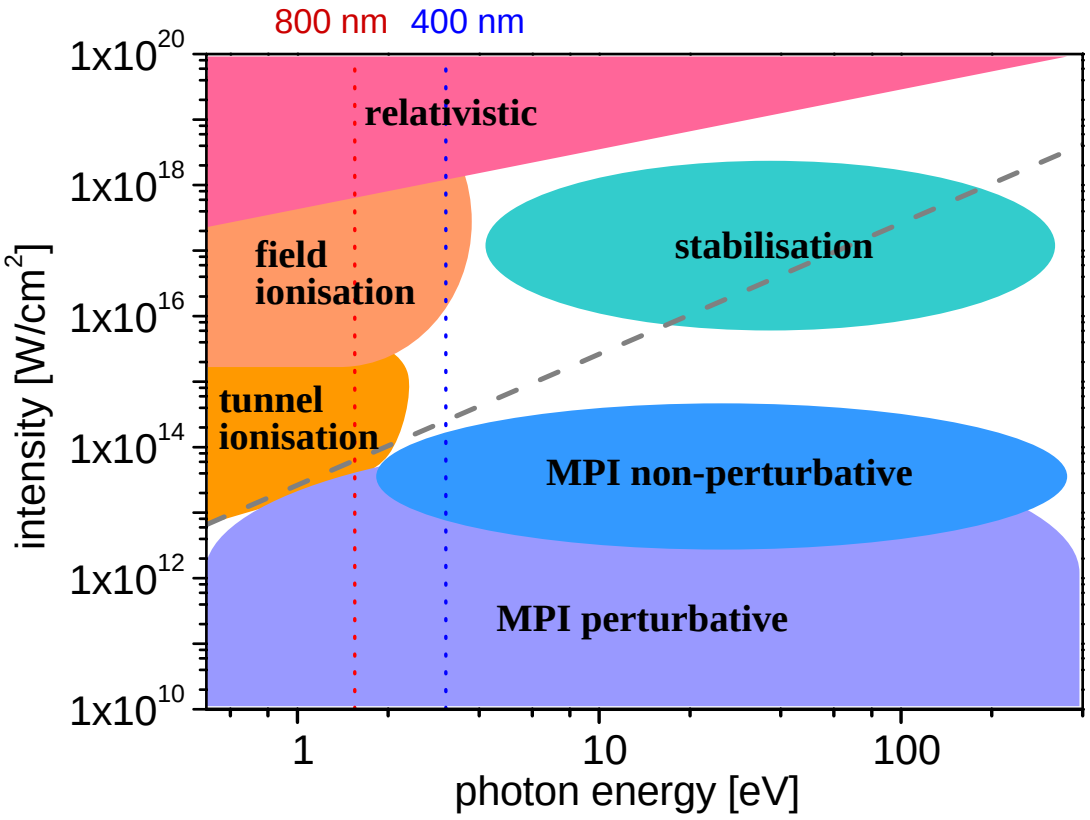

Figure 3.1: Different photoionisation regimes as a function of the laser intensity and photon energy. The vertical dotted red and blue lines indicate photon energies related to the laser wavelength of 800 nm and 400 nm, respectively. The dashed gray line shows case of $\gamma = 1$ for C_{60} ionisation which separates the multiphoton regime ($\gamma > 1$) from the tunnelling regime ($\gamma \ll 1$).

parameter can be interpreted as the ratio between the time required for tunnelling and the oscillation period of the laser radiation.

Different photoionisation regimes are schematically depicted in Fig. 3.1. For the rather low laser intensities ionisation proceeds either by a multiphoton perturbative process for the lowest intensities or a multiphoton non-perturbative process [MMa91]. If the laser frequency is quite low but the laser intensity is moderately strong, ionisation occurs via tunnelling [ASM89]. Field ionisation happens at even higher laser intensity when the potential barrier is completely suppressed by the laser field. Under certain conditions [PTV03] the stabilisation regime of photoionisation can be achieved [Rei01]. Finally, extremely hight laser intensities open an entirely new domain in atomic, plasma and nuclear physics, where relativistic effects play an important role [JKy03, KFS03, SHH06]. For example, the laser electric field corresponding to

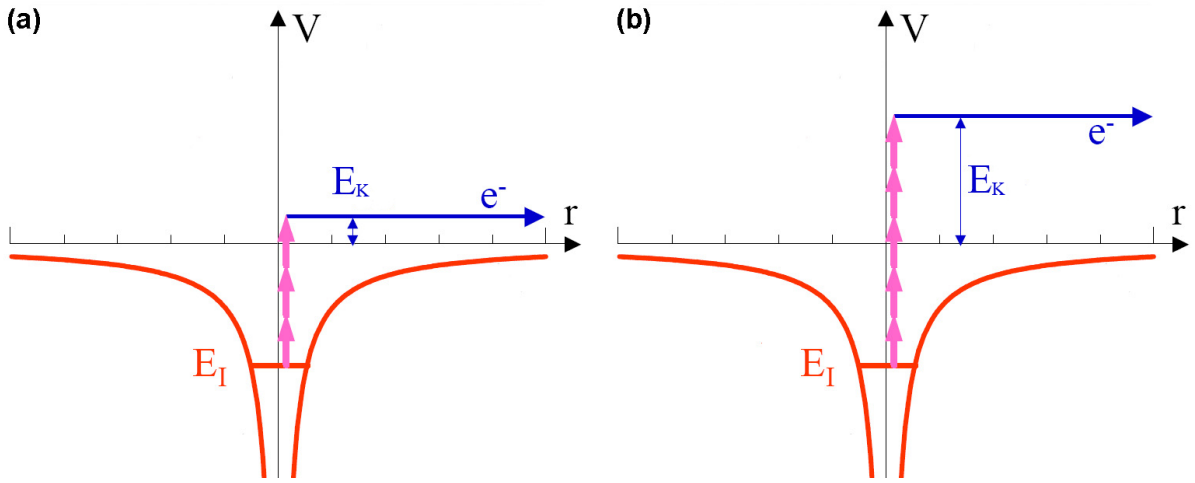

Figure 3.2: Perturbative nonlinear regime of ionisation ($\gamma > 1$): (a) multiphoton ionisation; (b) above threshold ionisation.

an intensity of $10^{19}\,\mathrm{W/cm^2}$ is nearly $10^{11}\,\mathrm{V/cm}$, a value dramatically exceeding the intraatomic field. The quiver energy of an electron reaches $1\,\mathrm{MeV}$ at $10^{19}\,\mathrm{W/cm^2}$ and $\lambda = 1053\,\mathrm{nm}$. This energy becomes comparable with the electron rest energy of $\approx 0.5\,\mathrm{MeV}$. Hence, the electron motion becomes relativistic.

The vertical dotted red and blue lines in Fig. 3.1 indicate photon energies of the laser radiation used in the present work with wavelength of $800\,\mathrm{nm}$ and $400\,\mathrm{nm}$, respectively. The maximal achievable intensities are up to $4 \times 10^{14}\,\mathrm{W/cm^2}$ and $6 \times 10^{13}\,\mathrm{W/cm^2}$ at $800\,\mathrm{nm}$ and $400\,\mathrm{nm}$, respectively. Therefore, with such laser parameters both multiphoton and tunnel regimes of ionisations are reachable. The dashed gray line shows case of $\gamma = 1$ for C_{60} ionisation which separates the multiphoton regime ($\gamma > 1$) from the tunnelling regime ($\gamma \ll 1$).

A schematic diagram of the MPI process is depicted in Fig. 3.2a. The ionisation rate of N-photon ionisation Γ_N is given by

$$\Gamma_N = \sigma_N I^N \quad , \tag{3.7}$$

where σ_N is the generalised cross-section for N-photon absorption and I the laser intensity. This expression leads to a linear dependence on a double logarithmic scale

$$\log \Gamma_N = N \log \sigma_N I \quad , \tag{3.8}$$

where the slope N indicates the number of photons required for ionisation according to Eq. (3.5). The ionisation rate in an MPI process strongly depends on the frequency of the

laser radiation due to possible resonances between the energy of several absorbed photons and the energy of some intermediate stationary state. In that case one speaks about resonance enhanced multiphoton ionisation (REMPI). If the field strength is strong enough, REMPI can be induced by the AC-Stark shift[1] of electronic states into resonance. Eq. (3.7) breaks down at some critical light intensity I_s, above which a change in intensity dependence is observed due a nearly 100% ionisation probability [LHM85]. This intensity I_s is called "saturation intensity".

At rather high intensities (but generally below I_s) an electron can absorb more photons than the minimum number N required for ionisation (see Eq. (3.5)), say $N+S$, as shown in Fig. 3.2b. In this case one speaks about "above threshold ionisation" (ATI) [AFM79]. In the range of moderate laser intensities Eq. (3.4) and Eq. (3.7) can be generalised in the ATI case to

$$E_K + E_{int} = (N+S)\hbar\omega - E_I \tag{3.9}$$

and

$$\Gamma_{N+S} \propto I^{N+S} \quad , \tag{3.10}$$

respectively. An ATI photoelectron spectrum consists of several peaks separated by $\hbar\omega$. With increasing laser intensity the ATI peaks corresponding to a higher number S of photons become more probable and do not necessarily follow the power law Eq. (3.10) [YPA86]. At the same time, the amplitude of low energy ATI peaks is reduced [KKM83].

At moderate laser intensities MPI can be well described by using of the lowest order perturbation theory (LOPT) with respect to the electron filed interaction [FPA82, PFA84]. This theory predicts the power law for the ionisation rate described by Eq. (3.7). Near resonant or resonant cases of MPI are the subject of an additional complexity for the theoretical description. However, the methods, which can handle these difficulties, have been developed [Fai87]. The perturbation theory breaks down for higher laser intensities since the involved atomic states undergo the AC-Stark shift and can not longer be considered as unperturbed [FBM87]. Qualitative, the non-perturbative nature of ATI is understood by using a simple approach [MAc89] based on the Keldysh model [Kel65].

In contrast, for $\gamma \ll 1$ (the laser radiation with high intensity and/or low frequency) the strong laser field distorts the potential energy surface of the atom such that a potential barrier

[1] The dynamical shifting of energy levels in atoms and molecules due to an applied electromagnetic field.

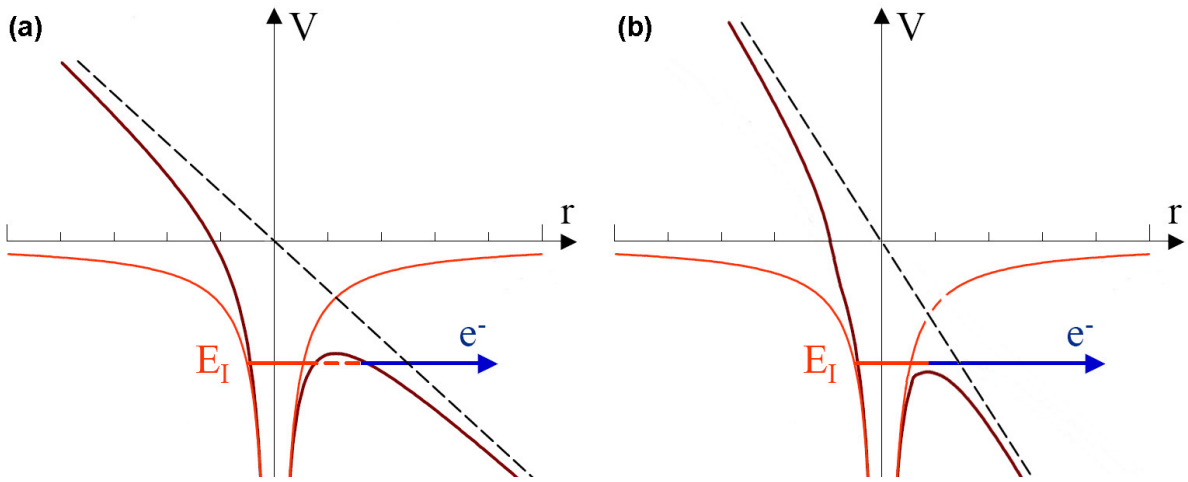

Figure 3.3: Strong field regime of ionisation ($\gamma \ll 1$): (a) tunnelling ionisation; (b) above barrier ionisation.

is formed. This is illustrated in Fig. 3.3a. The barrier divides a space into two regions where the electron is bound or free. A local maximum of the barrier is called the "saddle point". If the laser frequency is low enough, the electron can leave the atom by tunnelling through the potential barrier. This process is known as "tunnelling ionisation" [GHa98]. The rate of the tunnelling ionisation Γ_T has a simple exponential form

$$\Gamma_T \propto \exp\left[-\frac{2(2E_I)^{3/2}}{3\sqrt{I}}\right] \quad . \tag{3.11}$$

At even higher intensities, the laser radiation suppresses the potential barrier so far that the electron is able to escape freely from the atom as depicted in Fig. 3.3b. It happens when the saddle point reaches the electron binding energy. This is called "over the barrier ionisation" (OTBI) or the "barrier suppression ionisation" (BSI) [BRK93]. The threshold intensity of OTBI for hydrogen-like atoms is given by the following expression

$$I_{OTBI} = 4 \times 10^9 \frac{E_I^4}{Z^2} \quad , \tag{3.12}$$

where I_{OTBI} is the threshold intensity in W/cm^2, E_I is the binding energy of the electron in eV, and Z is the charge state of the relevant atom or ion. Since the orbital angular momentum of the initially bound electron is not taken into account in Eq. (3.12), it does not give correct results for complex atoms.

Assuming that the laser frequency is low it is possible to consider tunnelling within the framework of the quasi-static approximation [SPD90]. It is based on the assumption that the

tunnelling occurs in a fraction of an optical cycle at which the change of the electric field is negligible. This framework allows one to calculate the ionisation rates in an altering laser field using the static field ionisation rates. There are several theoretical approaches for an analytic calculation of static field ionisation rates. The oldest among them is so-called the "Keldysh theory" [Kel65, Fai73, Rei80]. The effect of the atomic Coulomb potential is neglected in the Keldysh theory. Such assumption is also known as the "strong filed approximation" (SFA). As a result, it underestimates the ionisation rates. In 1966 Perelomov, Popov, and Terent'ev developed a new method to calculate the ionisation probability (PPT theory) [PPT65]. According to the PPT theory the rate of the tunnelling ionisation with the linear polarised light for the hydrogen-like atom is

$$\Gamma_T = \sqrt{\frac{3n^3\sqrt{I}}{\pi}} \frac{(2l+1)(l+|m|)!2^{4n-2|m|-2}n^{-6n+3|m|}}{(n+l)!(n-l-1)!(|m|)!(l-|m|)!} \times \frac{\exp\left[-2/(3n^3\sqrt{I})\right]}{(\sqrt{I})^{2n-|m|-1}} \quad , \tag{3.13}$$

where n is the principal quantum number, l is the orbital angular quantum number, and m is the magnetic quantum number. Eq. (3.13) is valid only if the strength of the external electric field is weak compare to the atomic Coulomb potential. Twenty years later Ammosov, Delone, and Krainov developed the so-called "ADK theory" [ADK86]. The ADK theory is an extension of the PPT theory to the case of complex atoms and ions. The ADK theory gives the following ionisation rate for linearly polarised light

$$\Gamma_{ADK}^{lin} = \sqrt{\frac{3(n^*)^3\sqrt{I}}{\pi Z^3}} \frac{\sqrt{I}D^2}{8\pi Z} \exp\left[-\frac{2Z^3}{3(n^*)^3\sqrt{I}}\right] \quad , \tag{3.14}$$

where $n^* \equiv \frac{Z}{\sqrt{2E_I}}$ is the effective principal quantum number and $D \equiv \left(\frac{4eZ^3}{\sqrt{I}(n^*)^4}\right)^{n^*}$. The ionisation rates for the circular polarised light differ from the rates for the linear polarised light and have a more simple form

$$\Gamma_{ADK}^{circ} = \frac{\sqrt{I}D^2}{8\pi Z} \exp\left[-\frac{2Z^3}{3(n^*)^3\sqrt{I}}\right] \quad . \tag{3.15}$$

Eq. (3.14) and Eq. (3.15) have a restricted region of validity. For the laser intensities which are higher than I_{OTBI} the ADK theory increasingly overestimates the ionisation rate. This is due to the AC-Stark shift of the ground state. Indeed, the dynamic Stark effect caused by the laser field which may shift atomic and molecular energy levels in a significant manner. For molecules sufficiently strong fields can thus cause potential energy crossings and consequently lead to laser field induced non-adiabatic transitions, a subject of very active research in many

experimental and theoretical studies [LBR01, KSF03, KST04, MRS04]. Such behaviour will be most efficient if the laser frequency is close to a resonance of the system studied. Manifestations of the Autler-Townes splitting [ATo55] have long been known in studies of ATI processes [Lag93] and definitively need to be considered also for molecules in intense laser fields. According to estimations such splitting can be in the eV region at rather moderate intensities of $10^{11}\,\mathrm{W/cm^2}$, providing the laser frequency is in resonance with a transition of significant oscillator strength [HLS05].

All above described cases of nonlinear ionisation have been considered from the point of view of the single active electron (SAE) approximation [KSK92, XTL92, SJW95]. The SAE approximation assumes that only the single lowest bound electron interacts with the laser field and it is bound by an effective potential which reproduces the ground state and singly excited states. The dynamics of the remaining bound electrons is neglected in this approach. This approximation supposes that multiple ionisation happens only as a stepwise process. In reality, most of atoms and molecules have more than one electron. Nevertheless, the SAE approximation has been successfully used to describe experimental data in many cases. However, multielectron effects are essential for the explanation of many physical phenomena. They are especially important for the description of the photoinduced processes in large systems. Both theoretical [FKM03] and experimental [LBI02] works demonstrated that multiple active electrons (MAE) are excited in complex systems.

Several mechanisms of MAE response have been suggested. According to the collective tunnelling model there is an opportunity of the simultaneous tunnelling of two electrons [EDM00]. But the tunnelling rates predicted by this model are too low for the explanation of experimental data.

It was proposed that non-sequential ionisation may arise from the shake-off mechanism [FBC92]. The escape of the first electron changes the effective potential of the atomic core. The second electron can not adapt to this rapid change of the effective potential. It can be shaken and displaced from the atom as well. Unfortunately, this model does not give any dependence of ion yields on the laser polarisation and it fails to explain experimentally observed the spatial distribution of ejected electrons [FBC94].

Another classical model based on electron electron rescattering was suggested [Cor93]. According to this model the electron after tunnelling through the potential barrier acts as a

classical charged particle in the laser field. This electron is accelerated away from the ionic core and after about one half (or multiple) of an optical cycle is driven back when the laser filed changes its sign. The maximum value of the electron kinetic energy which can be acquired from the laser field is $3.17U_P$[1] [MSt99]. The electron may be scattered inelastically by the ion core, transferring part of its energy to another electron. Thus, a second electron may be ejected from the ionic ground state to the continuum. This process is called "non-sequential double ionisation" (NSDI) [WSD94, WGW00, WWS00]. Alternatively, the electron can be elastically scattered by the ion core. In this case, it can acquire drift energies much higher than otherwise[2]. Such effect is referred to as high order above threshold ionisation (HATI) [MPB03]. Finally, the electron can recombine with the ion emitting its energy in form of a high energy photon. This process is known as the "high harmonic generation" (HHG) [ZPM96, SKu97]. Presently, the rescattering model is commonly accepted as the mechanism for the non-sequential ionisation [MFS00, FMF01, WHC01].

Multiphoton excitation may also lead to a decay process (fragmentation) of an excited parent particle (molecule or cluster) to products which can be formulated as

$$parent \xrightarrow{N\hbar\omega} daughter + ejected\ particle \quad . \tag{3.16}$$

Usually, the daughter particle corresponds to the more heavy fragment, while the ejected particle is the rest. The energy balance of a decay process is

$$E_{init} + N\hbar\omega = E_b + E_d + \varepsilon^* + \varepsilon \quad , \tag{3.17}$$

where E_{init} is the initial internal energy of the parent particle before excitation, E_b is the binding energy of the ejected particle, E_d is the internal energy of the daughter particle after the decay, ε^* is the internal energy of the ejected particle, and ε is the kinetic energy released in the process. For fragmentation of a molecule (cluster) the excess energy $E_{int} = E_{init} + N\hbar\omega$ (see Eq. (3.4)) absorbed by the system must exceed the binding energy of the ejected particle ($E_{int} > E_b$). The released kinetic energy is distributed over the decay products in accordance with conservation of momentum and energy. The kinetic energy release distribution provides information concerning the system structure dynamics, and reaction energetics [Eng87].

[1] The maximum energy which the electron tunnelled with zero velocity can return to the core according to the classical model.

[2] For the electron backscattered by 180° the maximum acquire energy is $10.007U_P$.

A multiphoton absorption in large, finite systems besides the direct processes also may lead to delayed ionisation [OSi89, KCa98, LCP03] and fragmentation [SLe80, VCN96, GKD06]. Both processes demonstrate a statistical nature and occur on the long time scale after multiphoton excitation.

In addition to the excess energy, a so-called "kinetic shift energy" [Lif00] has to be deposited to observe C_{60} fragmentation on the time scale of nanoseconds to microseconds. Assuming that the total energy of the system is statistically distributed over the vibrational degrees of freedom, the kinetic shift energy is required to allow for channelling the necessary dissociation energy with sufficient probability into the coordinates involved in the bond breaking.

There are several theoretical approaches to describe statistical ionisation and fragmentation. The theory of the detailed balance [ABH02] takes its origin from the Weisskopf formalism [Wei37]. This theory was successfully applied to describe the delayed ionisation of highly excited sodium clusters [SKI01], fullerene anions [AHN02], and neutral C_{60} [HHC03, LBo04]. The rate of a unimolecular decay can also be calculated using the Rice-Ramsperger-Kassel (RRK) theory [RRa27, RRa28, Kas28a, Kas28b]. This theory assumes that the rate is proportional to the amount of the internal energy which is divided over all vibrational degrees of freedom. The application of the RRK theory is known for wide range of systems, namely, for polyatomic molecules [RKB81, SKS95], C_{60} fullerene [WLy92, EWC96], rare gas clusters [HIN94], metallic clusters, their cations, and anions [CPL97, KSW99, SSE00].

The accuracy of all statistical models is limited because the distribution of the internal energy as well as most of the parameters values used in the statistical models usually are exactly not known. Moreover, the observations in many cases of discrepancies between the statistical models and the experimental data [CAR93, YHW93] clearly indicate the evidence for the breakdown of the statistical equilibrium hypothesis.

3.3 Energy Redistribution

The flow of absorbed energy in bulk materials is relatively well understood for solid state systems [POg97, EPC00]. There is a number of relaxation processes such as electron-electron, electron-phonon, electron-plasmon, electron-photon, electron-impurity interactions and diffusion and ballistic transport into the bulk. Generally, electron-electron and electron-phonon

scattering are primary relaxation mechanisms [ONP97], therefore only these two relaxation channels are considered below. The relaxation processes in large, finite systems have been investigated in detail for a few model systems [LBW99, HMo00]. It was found that the relaxation processes in finite systems differ significantly from those in bulk materials.

The basic scheme of energy relaxation is depicted in Fig. 3.4. The laser energy is predominantly absorbed into the electronic system of a species which leads to a certain internal energy E_{int}. The corresponding electron distribution has non-thermal character. The first step of energy relaxation corresponds to the thermalisation of electrons by electron-electron coupling. One may distinguish two different approaches to describe this mechanism depending on the excitation density [LLB04]. For low excitation densities ($< 10^{-4}$ e^-/atom), when the excited electrons interact predominantly with the equilibrium part of the electron distribution, scattering rates can be estimated using the Fermi-liquid theory [EPC00]. For high excitation densities ($> 10^{-3}$ e^-/atom), when rapid thermalisation via multiple collisions among the excited non-equilibrium electrons may establish a Fermi-Dirac distribution and the concept of separate electron and phonon temperatures is valid, the well known "two temperature model" can be applied [Gad00]. The second important relaxation mechanism is energy transfer of the hot electrons to the lattice (in bulk materials) or coupling to the vibrational degree of freedom (in finite systems). This process is called "electron-phonon coupling" and it is characterised by a temperature exchange between electrons and phonons. Also surface effects have a significant influence on the relaxation processes in large, finite systems. On the other hand, the relaxation mechanisms described above can not be directly applied to very small clusters. In this case the discrete structure of electronic states is considered. C_{60} is a large but still finite molecular system, therefore the above mentioned approaches in the description of photophysical and photochemical processes have to be taken with a grain of salt.

Time-resolved photoemission studies on bulk material show that the time scale for the electron-electron coupling τ_{el} varies from 5 to ~ 500 fs [POg97]. It is also sensitive to the intensity and the frequency of the laser radiation used for investigations. The characteristic times for the electron-phonon coupling τ_{ph} lie on the time scale between 1 and 5 ps [KSR98]. In molecules, such as C_{60}, these processes occur on much faster time scales ($\tau_{el} < 70$ fs, $\tau_{ph} = 200 - 300$ fs). However, both relaxation processes may be considered to occur sequentially.

The standard theoretical approach for the electron-electron coupling is the Landau theory

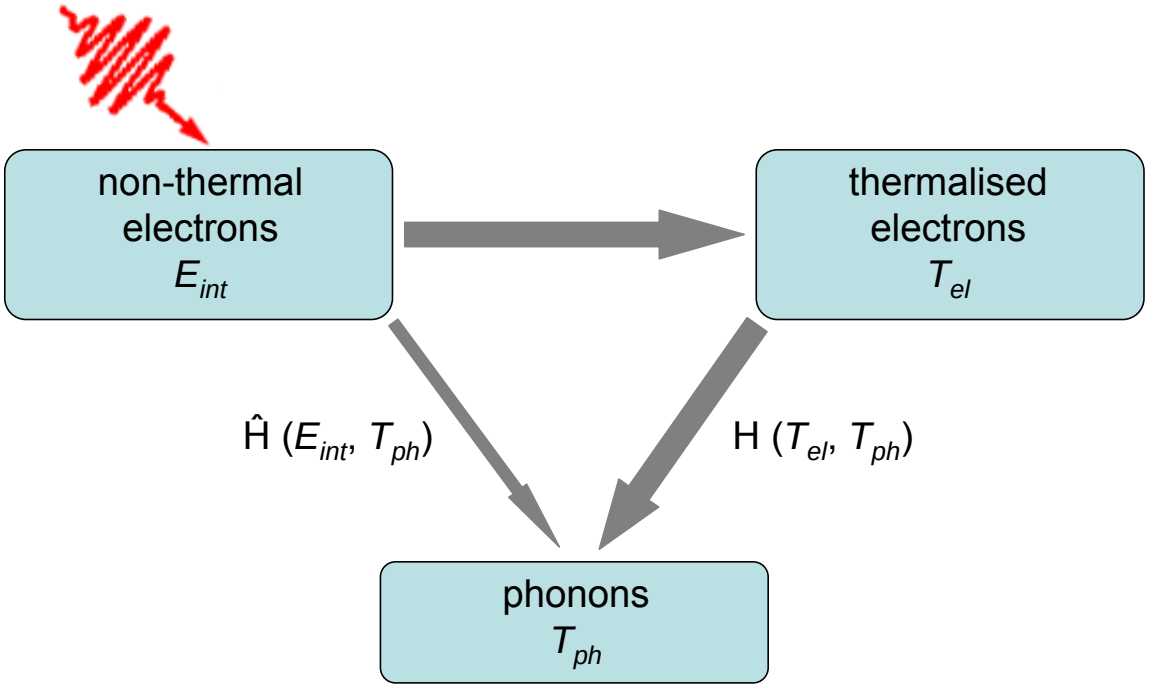

Figure 3.4: Illustration of energy relaxation processes in large but finite systems.

of the Fermi liquid (LTFL) [PCa73]. This theory predicts characteristic time constants of electron-electron scattering τ_{el} near the Fermi level in a free-electron gas based on its electron density. τ_{el} is determined by the available phase space between the electron energy E and the Fermi level E_F and it is given by [SKB99]

$$\tau_{el} = \tau_0 \left(\frac{E_F}{E - E_F} \right)^2 \tag{3.18}$$

with

$$\tau_0 = \frac{128}{\pi^2 \sqrt{3} \omega_p} \quad , \tag{3.19}$$

where ω_p is the plasmon frequency. At energies higher than the plasmon energy $\hbar\omega_p$, electron-plasmon interaction becomes important [XCM96]. Eq. (3.18) gives only the lower limit of the electron-electron scattering time constant in real materials because the approximations used to obtain this expression tend to overestimate the electron-electron interaction even in a free electron metal, and since the plasma frequency in a real metal is screened by both virtual valance band excitations and the ionic nuclear cores [POg97]. Moreover, Eq. (3.18) does not include any band structure effects. For example, theoretical calculations of the electron dynamics in metals demonstrate that band structure effects can lead to a substantial deviation

of electron-electron scattering time constants from the prediction of the Landau theory of the Fermi liquid [SKB99].

Experimental observations of the electron-electron interaction in non-metals and finite systems demonstrated the mismatch with the Landau theory. In this case the following empirical expression for τ_{el} was suggested [XCM96, HMo00]

$$\tau_{el} = (E - E_F)^{-n} \quad , \tag{3.20}$$

where the constant n is 1 as it was found for graphite [XCM96] or 1.5 for carbon nanotubes [HMo00]. Such deviation arises from the reduction of the dimensionality and increasing influence of the electron-plasmon interactions.

The electron-phonon coupling can be described within the framework of the two temperature model [HWG00]. In this model, the electron and phonon baths are coupled by the electron-phonon coupling constant and the energy flow between these baths is given by two differential equations. The classical two temperature model is valid only after full electron thermalisation. For the correct description of the dynamics on the time scale before electron thermalisation completed the two temperature model can be extended by taking into account reduced electron-phonon coupling of non-thermalised electrons (thin arrow in Fig. 3.4) [LLB04].

C_{60} fullerene is a large but still finite molecular system with discrete energy levels and a well defined number of 274 modes for nuclear motion. Therefore, parameters such as "electron temperature", "phonon temperature", or "heat capacity" and the two temperature model wholly have a restricted application for the description of photophysical and photochemical processes in C_{60}. Moreover, one would rather tend not to attribute experimentally observed relaxation times in C_{60} to electron-electron coupling exclusively. Rather, highly excited electrons formed during an intense laser pulse will exchange energy by the combined action of electron-electron scattering and electron coupling with the various nuclear degrees of freedom of the neutral C_{60}.